Desalination and Water Treatment
www.deswater.com
doi: 10.5004/dwt.2021.27702

236 (2021) 45–54
October

Experimental design applied to improve the efficiency and the performance of the reverse osmosis process

Abdelilah Fatni[a,*], Abdellatif El Hammadi[a], Rachid Bouaddi[a], Abdelaziz Ait Taleb[a], Noureddine El Baraka[a], Abdellatif Laknifli[b]

[a]*Laboratory of Biotechnology, Materials, and Environment, Physicochemistry of Natural Environments, Materials, and Environment Team, Polydisciplinary Faculty of Taroudant, University Ibn Zohr, Taroudant, Morocco, Tel. +212 639647034; emails: abdelilah.fatni@gmail.com (A. Fatni), a.hammadi@uiz.ac.ma (A. El Hammadi), rach.bouaddi@gmail.com (R. Bouaddi), a.aittaleb@uiz.ac.ma (A. Ait Taleb), barakanour@gmail.com (N. El Baraka)*

[b]*Laboratory of Biotechnology, Materials, and Environment, Physicochemistry of Materials, Catalysis, and Valorization of Natural Resources Team, Faculty of Sciences, University Ibn Zohr, Agadir, Morocco, email: a.laknifli@uiz.ac.ma*

Received 26 November 2019; Accepted 2 August 2021

ABSTRACT

This research focuses on optimizing the reverse osmosis process applied to water desalination in the Noor 1 Ouarzazate plant. The purpose of this process is to remove salt from brackish water from the Mansour Eddahbi dam. A complete factorial design based on four factors, that is, 2^4, has been used to evaluate the parameters affecting the desalination efficiency aiming to optimize the conductivity rejection rate, the calcium rejection rate, the magnesium rejection rate, and the transmembrane pressure. Furthermore, a linear mathematical model based on the experimental results has been carried out to estimate the impact of the different parameters considered and their relative interactions. As a result, this study reaches the optimal conditions for the reverse osmosis process, pH is 8, the antiscalant concentration is 6 ppm, the flow rate is 38 $m^3 h^{-1}$, and the redox potential is 100 mV. It also shows that the pH, the antiscalant concentration, and the flow rate are the most statistically significant factors affecting the selectivity of metal ions, while the flow rate is the most influencing factor on the transmembrane pressure. Thus, the results of experience are applied to the process and verify the predicted optimal conditions.

Keywords: Noor 1 Ouarzazate; Water desalination; Reverse osmosis; Metal ions removal; Design experimental

1. Introduction

Over the last few decades, the available water resources have decreased due to excessive consumption [1,2]. To solve this issue, seawater or brackish water desalination is one of the most promising methods for producing freshwater [3–5].

Among the different desalination technologies, reverse osmosis (RO) is one of the leading filtration techniques currently available [3,5,6]. It is a demineralization process based on a semi-permeable membrane to remove the low molecular weight compounds from water [7,8]. Under the effect of a pressure gradient, which allows having two fractions with different concentrations, the first one that passes through the membrane is called permeate, and the second one, which is rejected, is called the concentrate [6,9].

The reverse osmosis applications are numerous. It is used for brackish water treatment, drinking production, seawater desalination, a ruse of wastewater, and industrial process water [6,10,11]. Moreover, reverse osmosis is often used to produce ultrapure water in the solar power plant [12,13].

Noor 1 is a good example. It is the first project within the solar energy complex of Ouarzazate City. It uses a parabolic concentrating solar power (CSP) technology with

* Corresponding author.

a capacity of 160 MW. The First National Operation & Maintenance Company (NOMAC) operates it [14–16].

This technology used in the plant consists of solar radiation that is concentrated by curved mirrors on a tube or collector through which a heat transfer fluid (HTF) circulates [17–19]. Then, the liquid is used to collect the heat as thermal energy, transport it to the steam generation system (SGS), and generate electricity through a turbine generator [13,19–21].

Water remains an essential element during this process. Therefore, effective treatment is required to remove all undesirable substances in order to obtain demineralized water [17,22].

Water pretreatment includes hypochlorite disinfection, coagulation-flocculation, dissolved air flotation, and multimedia system [23,24]. Demineralization of water goes through three essential steps, it begins with the first reverse osmosis 1 (RO1), followed by the second reverse osmosis (RO2), and it ends with electrodeionization (EDI) [14,25,26].

Improving the quality of demineralized water requires enhancing the quality of each step of the process [26]. In this study, particular emphasis is placed on the first step (RO1), considered a decisive stage in the treatment process. In order to evaluate and improve the efficiency of this process, it has been relying on an experimental design.

The experimental design is the set of specific experiments determined by a matrix composed of at least two factors and a minimum of two levels; it should be developed to obtain the responses [27,28]. The number of experiments and the levels of the factors studied depends on the established matrix. In addition, it allows a more accurate description of the process by considering the possible interactions between the different factors affecting the process [3,29].

Firstly, the physicochemical composition of the feed water, the permeate, and the concentrate has been analyzed. Secondly, an experimental design methodology based on four factors, the pH, the flow rate, the concentration of antiscalant, and the redox potential, has been developed to detect their optimum condition. Finally, this model optimizes conductivity rejection rate, calcium rejection rate, magnesium rejection rate, and transmembrane pressure.

2. Materials and methods

The experiment was carried at the water treatment plant (WTP), Noor 1 plant Ouarzazate City, to evaluate the efficiency and improve the performance of the reverse osmosis process for metal ions removal from the water.

2.1. Feedwater

The source of the water supply for the solar power station is the dam Mansour Eddahbi. The feed water reaches the first reverse osmosis membrane (RO1) after undergoing pretreatment and primary treatment; screening, sandblasting, coagulation–flocculation, dissolved air flotation (DAF), and multimedia filtration [14,15,24].

Reverse osmosis RO1 consists of three trains installed in parallel. Each train is composed of two stages; the feedwater passes through the first stage (made up of four modular series), and the rejection is filtered again through the second stage (consisting of three modular series) [14]. All the experiments were done on the first train of RO1.

2.2. Membrane treatment

The type of membrane used in each modular of reverse osmosis 1 was Filmtec BW30XFR-400/34i. Its specifications are shown in Table 1 [12,30]:

2.3. Chemicals reagents

The feedwater used for the desalination process is conditioned by adding a certain number of chemicals to improve downstream processing performance. The antiscalant with the commercial name Hypersperse MDC704, based on phosphonate [31], avoids scaling. Hydrochloric acid avoids scaling and setting the pH. The antifouling, SMAS Y-230, prevents biofouling. Moreover, the reducing agent, sodium bisulfite, removes residual free chlorine [14,25].

2.4. Analytical methods

The ion concentrations in the feedwater, the reverse osmosis permeate and concentrate solutions were measured using an analytical kit, HACH Reagents, using the DR3900 Laboratory VIS Spectrophotometer with RFID technology. A pH meter HQD Portable was used for pH measurements of the solution throughout the study. The electrical conductivity and the total dissolved solids (TDS) are measured by HQD Portable Meters. In addition, measuring and monitoring turbidity was carried out with a 2100Q Portable Turbidimeter.

2.5. Data analysis

2.5.1. Efficacy evaluation

The evaluation of the efficiency of treatment by the reverse osmosis (rejection rate) is calculated by the following formula [9,11]:

$$R(\%) = \left(\frac{C_0 - C_P}{C_0}\right) \times 100 = \left(1 - \frac{C_P}{C_0}\right) \times 100 \quad (1)$$

where R: rejection rate, also called selectivity; C_0: concentration of the species present in the feedwater (ppm); C_P: concentration of the same species in permeate water (ppm); C_R: concentration of the same species in concentrate water (ppm).

The membrane flux is calculated using Eq. (2) [32]:

$$J_p = \frac{F_p}{A} \quad (2)$$

The recovery rate R_r of the reverse osmosis is calculated by Eq. (3) [11]:

$$R_r(\%) = \frac{F_P}{F_0} \times 100 \quad (3)$$

the mass of scale formed on the membrane surface can be calculated using the following mass balance [32]:

Table 1
Specifications of the reverse osmosis 1 (RO1) membrane

Brand	Model	Membrane type	Active area (m^2)	Average salt rejection (%)	Minimum salt rejection (%)
FILMTEC Membranes	BW30XFR-400/34i	Polyamide thin-film composite	37	99.65%	99.40%
Max. pressure (bar)	Max. temperature (°C)	Permeate flow ($m^3 h^{-1}$)	pH range, continuous operation	Maximum feed silt density index	Free chlorine tolerance
41	45.0	43.3	2–11	5	<0.1 ppm

$$M_t = \left(J_0 \times C_0\right) - \left(J_P \times C_P + J_R \times C_R\right) \quad (4)$$

where A: active area of membrane (m^2); $M_{t/s}$: mass of scale formed on the membrane surface per unit of time (g m^{-2} h^{-1}); J_0: Flow of water in the feed stream (L m^{-2} h^{-1}); J_P: the flow of water in the permeate stream (L m^{-2} h^{-1}); J_R: the flow of water in the concentrate stream (L m^{-2} h^{-1}).

2.5.2. Optimization method

A model based on experimental design methodology is used to evaluate the effect of parameters influencing the efficiency of the reverse osmosis process, using STATGRAPHICS Centurion XVI software [3].

The experimental design established is the two-level complete factorial design 2^n, where the factor number n is equal to four; pH (X_1), antiscalant concentration (X_2), flow (X_3), and redox (X_4). Thus, this experimental design matrix has two levels (–1 and 1) and sixteen experiments [3,27].

In this study, four responses were taken into account: conductivity rejection rate (Y_1), calcium rejection rate (Y_2), magnesium rejection rate (Y_3), and transmembrane pressure (Y_4).

Tables 2 and 3 show the experimental domain of the design with values for each factor used in the complete factorial design as well as the low and high levels studied and the goal of each response measured.

The experimental design model is an equation that correlates the response of a plan with the experimental factors studied [3]; it is 2-factor interaction with 11 coefficients. The regression equation with four parameters and their interactions is as follows:

$$Y_i = a_{i0} + a_{i1}X_1 + a_{i2}X_2 + a_{i3}X_3 + a_{i4}X_4 + a_{i12}X_1X_2 + a_{i13}X_1X_3 + a_{i14}X_1X_4 + a_{i23}X_2X_3 + a_{i24}X_2X_4 + a_{i34}X_3X_4 \quad (5)$$

where a_{i0}, a_{i1}, a_{i2}, a_{i3}, a_{i4}, a_{i12}, a_{i13}, a_{i14}, a_{i23}, a_{i24}, and a_{i34} are regression coefficients for each response.

3. Results and discussion

3.1. Water analysis

Feed, permeate and concentrate water were analyzed for six weeks (six samples each) from 23/10/2017 to 27/11/2017. The sample was taken every week. The flow rates are 53, 39.5, and 13.5 m^3 h^{-1}, respectively, with a rejection rate of 74.5% during operation.

3.1.1. Physical parameters

Physical parameters monitored are temperature, pH, conductivity, and turbidity as shown in Fig. 2.

The mass of scale of TDS formed on the membrane surface of each sample is presented in Table 4 using Eq. (4).

3.1.2. Chemical parameters

Chemical parameters monitored are calcium, magnesium, sulfate, iron, chloride, and orthophosphates, as shown in Fig. 3.

Table 2
Definition of experimental factors

Coded (X_i)	Factor	Range level	
		Min. value (–1)	Max. value (+1)
X_1	pH	7	8
X_2	Antiscalant concentration, ppm	0	6
X_3	Flow rate, m^3 h^{-1}	39	41
X_4	Redox potential, mV	50	100

Table 3
Definition of the responses measured

Coded (Y_i)	Responses	Goal
Y_1	Conductivity rejection rate, %	Maximize
Y_2	Calcium rejection rate, %	Maximize
Y_3	Magnesium rejection rate, %	Maximize
Y_4	Transmembrane pressure, bar	Minimize

The average temperature of the water varies between 19°C and 25°C, which is decreased in the last two samples because of the low temperature these days. The pH of the feed water ranges from 7.1 to 7.2. The turbidity at the inlet of the membranes is generally greater than 1 NTU, which leads to very rapid organic clogging of the membranes due to colloidal material, thus reducing their yield. This high value is mainly due to the pretreatment not put into service. The conductivity of feedwater is about 1680 and 43.4 µs cm^{-1} for permeate water; the average efficiency is 97.54%.

From the above results, we will deduce that the major elements present in water with high concentrations are calcium, magnesium, chloride, and sulfate. On the other hand, iron and orthophosphates are present at low concentrations. Therefore, the average rejection rates for eliminating major ions in water are 99.652% for calcium, 99.656% for magnesium, 97.522% for sulfate, and 97.295% for chloride.

3.2. Optimizing the performance

3.2.1. Experimental results

The performance can be improved by looking for optimal conditions for all parameters using the experimental design method. Table 5 shows a worksheet containing the 16 experiments performed in the order they were executed, and each sample was taken after 10 min of flushing and 4 h of operation.

From these experiments, it is noted as a preliminary remark that the pH 8 and antiscalant concentration of 6 ppm gives the best retention, and the flow rate of 38 m^3 h^{-1} gives a low transmembrane pressure.

Table 4
The mass of scale of TDS

Date	TDS (ppm)			(TDS × J) (g m^{-2} h^{-1})			M_t (g m^{-2} h^{-1})
	Feed	Permeate	Concentrate	Feed	Permeate	Concentrate	
23/10	1,170	31.38	4,291	39.90	0.80	37.28	1.83
30/10	1,177	29.52	4,306	40.14	0.75	37.41	1.98
06/11	1,181	21.80	4,383	40.28	0.55	38.08	1.65
13/11	1,180	22.73	4,396	40.24	0.58	38.19	1.48
20/11	1,189	26.22	4,404	40.55	0.67	38.26	1.63
27/11	1,192	24.40	4,337	40.65	0.62	37.68	2.36
Average	1,182	26.01	4,353	40.30	0.66	37.81	1.82

Table 5
Worksheet for experiments

Exp. no.	Factors				Responses			
	X_1: pH	X_2: antiscalant	X_3: flow	X_4: redox	Y_1: conductivity rejection	Y_2: calcium rejection	Y_3: magnesium rejection	Y_4: transmembrane pressure
		ppm	m^3 h^{-1}	mV	%	%	%	bars
1	8.0	0.0	38.0	100.0	98.691	99.756	99.754	6.06
2	8.0	6.0	41.0	50.0	98.736	99.783	99.765	6.79
3	7.0	6.0	41.0	100.0	98.110	99.712	99.728	6.59
4	7.0	0.0	41.0	100.0	98.148	99.685	99.718	6.67
5	7.0	6.0	38.0	50.0	98.074	99.714	99.726	6.33
6	7.0	0.0	38.0	100.0	98.007	99.718	99.719	6.11
7	7.0	6.0	41.0	50.0	98.185	99.716	99.739	6.76
8	8.0	0.0	41.0	50.0	98.651	99.734	99.750	6.77
9	8.0	6.0	41.0	100.0	98.749	99.797	99.760	6.82
10	8.0	6.0	38.0	50.0	98.738	99.781	99.758	6.42
11	7.0	0.0	41.0	50.0	98.152	99.693	99.738	6.79
12	7.0	0.0	38.0	50.0	98.077	99.702	99.714	6.15
13	7.0	6.0	38.0	100.0	98.111	99.724	99.725	6.13
14	8.0	6.0	38.0	100.0	98.702	99.783	99.761	6.32
15	8.0	0.0	38.0	50.0	98.566	99.752	99.757	6.06
16	8.0	0.0	41.0	100.0	98.688	99.741	99.735	6.42

3.2.2. Analyze the experimental results

According to the complete factorial design for responses, estimated effects, standard errors, variance inflation factor (VIF), sum of squares (SS), degree of freedom (Df), mean square (MS), *F*-ratios, and *P*-values, standardized effects are calculated in Table 6.

The ANOVA table shows the significate (standardized) effects of each response. The effect's statistical significance can be tested by comparing the MS against an estimate of the experimental errors. It is significant if the *P*-value is lower than *F*-ratio and less than 5%, indicating that it is significantly different from zero at the 95.0% confidence level, except the main effects involved in significant interactions. Models have *P*-values below 5%, indicate that the model as the fit is statistically significant. The standardized effects are well illustrated on the Pareto chart.

3.2.3. Standardized effects and the Pareto chart

The Pareto graph is frequently used to evaluate the results of experimental designs. The effects of the factors and their interactions are presented as standardized effects (SE). Besides, a vertical line is drawn to show the factors and interactions that are significant. The red line on the *x*-axis corresponds to the critical value to indicate the minimum level [27].

Fig. 4 shows that the parameters influencing the conductivity rejection are pH, flow rate, and antiscalant. The parameters influencing the calcium rejection are pH, antiscalant, flow, pH-antiscalant interaction, and antiscalant-flow interaction. The parameters affecting the magnesium rejection are pH, antiscalant, and pH-flow interaction. The parameters influencing the transmembrane pressure are flow and antiscalant.

Table 6
Statistical parameters and analysis of variance

Analyze experiment	Effect	Estimate	Standard error	VIF	SS	Df	MS	*F*-ratio	*P*-value
Y_1: conductivity rejection	Average	98.3991	0.0109	–	–	–	–	–	–
	X_1	0.5821	0.0217	1	1.3555	1	1.3555	718.82	0.0000
	X_2	0.0531	0.0217	1	0.0113	1	0.0113	5.99	0.0308
	X_3	0.0566	0.0217	1	0.0128	1	0.0128	6.80	0.0229
	Total error	–	–	–	0.0226	12	0.0019	–	–
	Total (corr.)	–	–	–	1.4022	15	–	–	–
Y_2: calcium rejection	Average	99.7369	0.0017	–	–	–	–	–	–
	X_1	0.0579	0.0033	1	0.0134	1	0.0134	301.00	0.0000
	X_2	0.0286	0.0033	1	0.0033	1	0.0033	73.63	0.0000
	X_3	–0.0086	0.0033	1	0.0003	1	0.0003	6.68	0.0272
	X_1X_2	0.0116	0.0033	1	0.0005	1	0.0005	12.14	0.0059
	X_2X_3	0.0101	0.0033	1	0.0004	1	0.0004	9.21	0.0126
	Total error	–	–	–	0.0004	10	0.00004	–	–
	Total (corr.)	–	–	–	0.0184	15	–	–	–
Y_3: magnesium rejection	Average	99.7404	0.0013	–	–	–	–	–	–
	X_1	0.0291	0.0026	1	0.0034	1	0.0034	128.82	0.0000
	X_2	0.0096	0.0026	1	0.0004	1	0.0004	14.07	0.0045
	X_3	0.0024	0.0026	1	0.0000	1	0.0000	0.86	0.3788
	X_4	–0.0059	0.0026	1	0.0001	1	0.0001	5.24	0.0478
	X_1X_3	–0.0074	0.0026	1	0.0002	1	0.0002	8.26	0.0184
	X_3X_4	–0.0069	0.0026	1	0.0002	1	0.0002	7.18	0.0252
	Total error	–	–	–	0.0002	9	0.00002	–	–
	Total (corr.)	–	–	–	0.0046	15	–	–	–
Y_4: transmembrane pressure	Average	6.4494	0.0211	–	–	–	–	–	–
	X_1	0.0163	0.0422	1	0.0011	1	0.0011	0.15	0.7081
	X_2	0.1413	0.0422	1	0.0798	1	0.0798	11.21	0.0074
	X_3	0.5038	0.0422	1	1.0151	1	1.0151	142.64	0.0000
	X_4	–0.1188	0.0422	1	0.0564	1	0.0564	7.93	0.0183
	X_1X_2	0.1188	0.0422	1	0.0564	1	0.0564	7.93	0.0183
	Total error	–	–	–	0.0712	10	0.0071	–	–
	Total (corr.)	–	–	–	1.2799	15	–	–	–

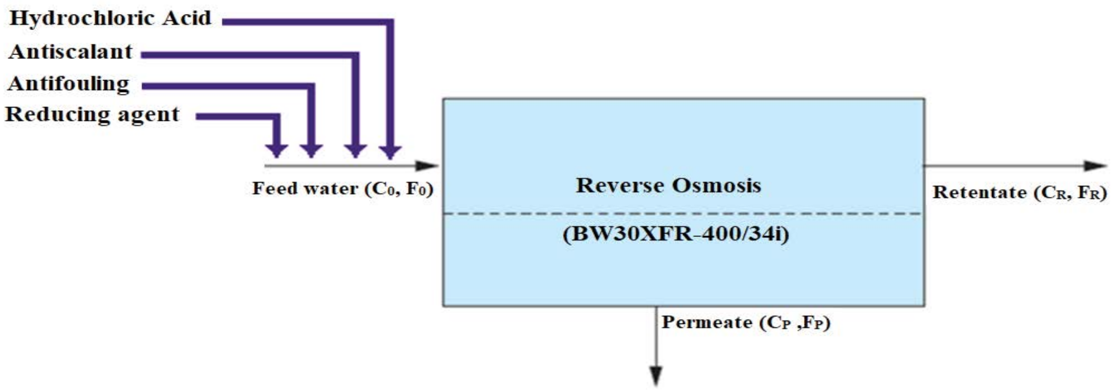

Fig. 1. Reverse osmosis filtration system.

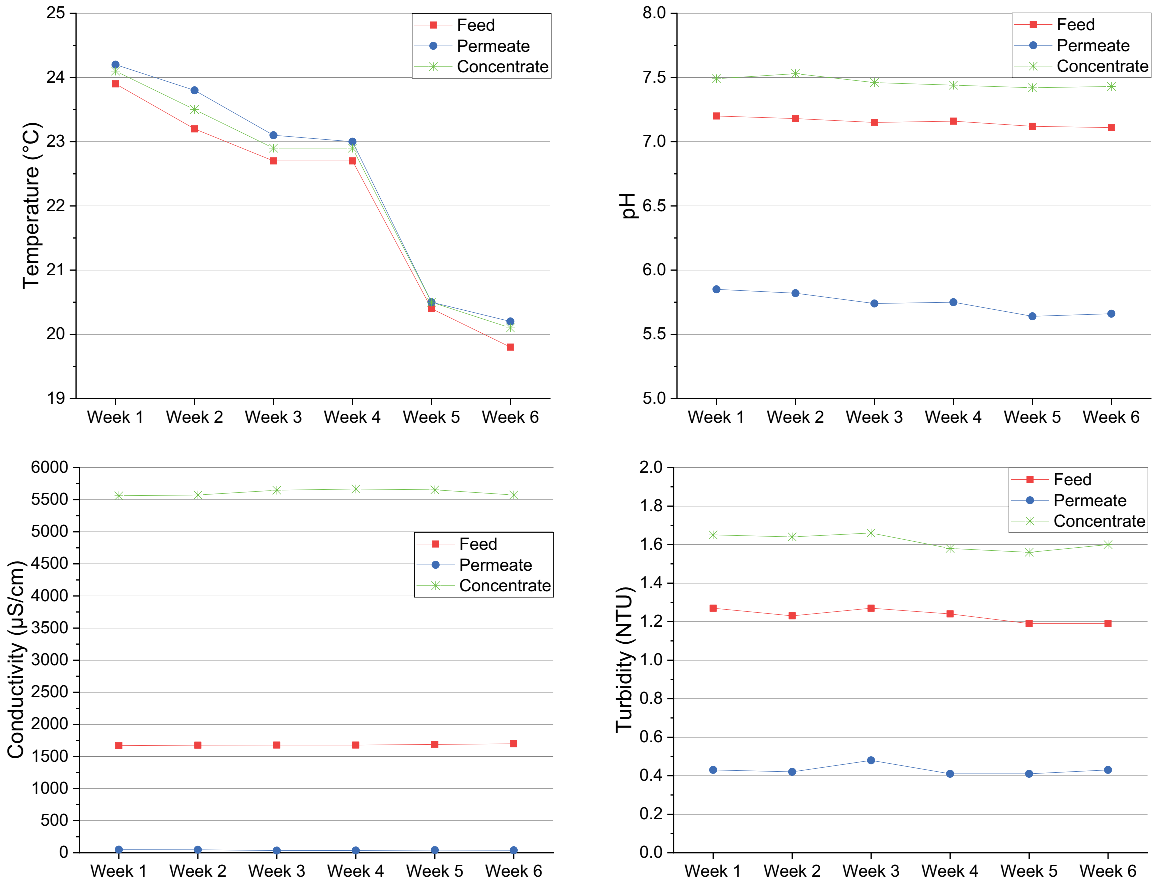

Fig. 2. Physical parameters (temperature, pH, conductivity, turbidity).

The main parameters affecting the desalination system respectively are pH, antiscalant concentration, flow rate, and redox potential.

3.2.4. Model equation for 2⁴ design

The factorial design allows the calculation of the effects of the factors and their interactions. This tool also allows a preliminary evaluation of the factors based on the generation of linear models [3]. In terms of coded variables, the model could be expressed using the regression models of the four responses by the following equations:

$$Y_1(\%) = 93.261 + 0.582125X_1 + 0.00885417X_2 + 0.018875X_3 \quad (6)$$

$$Y_2(\%) = 99.6226 + 0.04625X_1 - 0.0687292X_2 - 0.00625X_3 + 0.003875X_1X_2 + 0.001125X_2X_3 \quad (7)$$

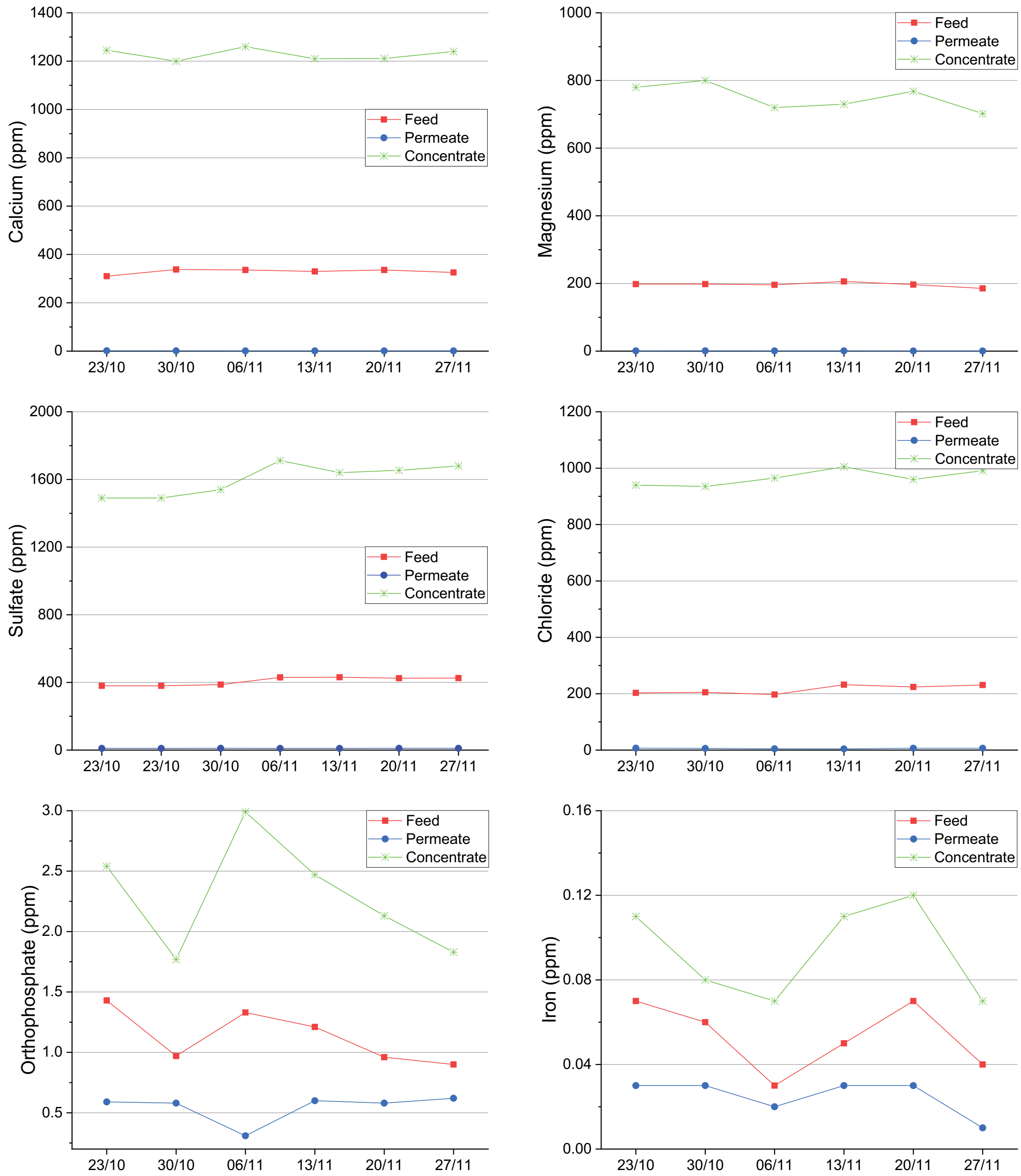

Fig. 3. Chemical parameters (calcium, magnesium, sulfate, chloride, orthophosphate, iron).

$$Y_3(\%) = 97.7666 + 0.223333X_1 + 0.00160417X_2 + 0.0445417X_3 + 0.00350333X_4 - 0.00491667X_1X_3 - 0.0000916667X_3X_4 \quad (8)$$

$$Y_4(\%) = 0.692917 - 0.1025X_1 - 0.273333X_2 + 0.167917X_3 - 0.002375X_4 + 0.0395833X_1X_2 \quad (9)$$

3.2.5. Optimize the responses

According to the study, the optimal setting of the experimental factors is determined. The results are displayed in Table 7.

Through the linear models, Table 8 shows the values of the responses at optimum.

The value of the responses, Y_1, Y_2, and Y_3, shows that the rejection rate is increased from 97.540%, 99.650%, and 99.660%, to 98.688%, 99.785%, and 99.762%, respectively. Similarly, they show that the transmembrane pressure is decreased from 6.581 to 6.276 bars.

4. Conclusion

In this study, the performance of the reverse osmosis process is investigated, and it is improved using the experimental design. Primary findings drawn can be summarized as follows:

- The components found in the water with high concentrations are calcium, magnesium, chloride, and sulfate.
- The pH and antiscalant concentration are the most significant parameters of the rejection rate of calcium, magnesium, and conductivity. The flow is the main parameter influencing the transmembrane pressure.
- The rejection rate of calcium and magnesium is increased from 98.650% to 99.785% and from 99.660% to 99.762%, respectively. The conductivity rejection rate is increased from 97.540% to 98.688%, and the transmembrane pressure is reduced from 6.58 to 6.276 bars.
- The optimal conditions obtained for the factors are: antiscalant concentration = 6 ppm, pH = 8, Flow rate = 38 $m^3 h^{-1}$, and redox potential = 100 mV. These parameters are validated by the results of the experiments applied to the process.

Table 7
Factor settings at optimum

Factor	Value
X_1: pH	8
X_2: Antiscalant concentration (ppm)	6
X_3: Flow rate ($m^3 h^{-1}$)	38
X_4: Redox potential (mV)	100

Acknowledgments

The authors would like to acknowledge the National Center for Scientific and Technical Research, Morocco, for its financial support through the Excellence Research Award. In addition, sincere thanks are extended to the industry partner to this research NOMAC for the technical and material support required to complete this study. In

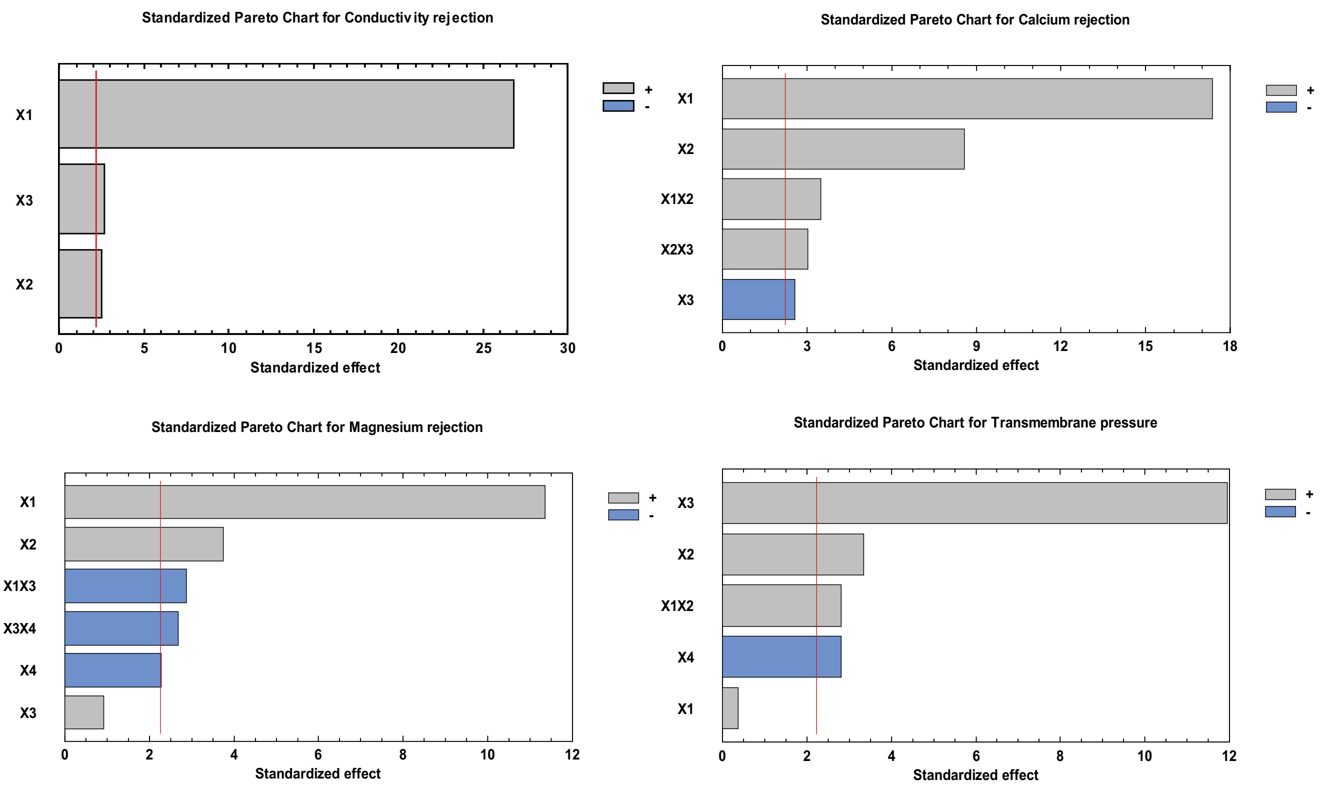

Fig. 4. Analysis of experiences (Pareto chart).

Table 8
Response values at optimum

Response	Optimized	Prediction	Lower 95.0% limit	Upper 95.0% limit	Desirability
Conductivity rejection: Y_1	yes	98.6884	98.6411	98.7357	0.9183
Calcium rejection: Y_2	yes	99.7852	99.7761	99.7944	0.8951
Magnesium rejection: Y_3	yes	99.7628	99.7551	99.7705	0.9571
Transmembrane pressure: Y_4	yes	6.2763	6.1612	6.3914	0.7054

particular, the authors would like to thank NOMAC operators located at the Noor 1 water treatment plant for providing valuable input data for the model.

Declaration of competing interest

The authors declare that they have no known competing financial interests or personal relationships that could have appeared to influence the work reported in this paper.

Symbols

a_0, a_1, a_2, a_3, a_4	—	Linear coefficient
$a_{12}, a_{13}, a_{14}, a_{23}, a_{24}, a_{34}$	—	Second-order interaction terms
ANOVA	—	Analysis of variance
C_0	—	Concentration of the species in the feedwater
C_P	—	Concentration of the species in the permeate water
C_R	—	Concentration of the species in the concentrate water
CSP	—	Concentrating solar power
EDI	—	Electrodeionization
DAF	—	Dissolved air flotation
Df	—	Degree of freedom
F_0	—	Flow of water in the feed stream
F_P	—	Flow of water in the permeate stream
F_R	—	Flow of water in the concentrate stream
HTF	—	Heat transfer fluid
MS	—	Mean square
M_t	—	Mass of scale formed on the membrane surface
pH	—	Potential hydrogen
R	—	Rejection rate
Redox	—	Oxidation/reduction potential
RO	—	Reverse osmosis
R_r	—	Recovery rate of the reverse osmosis
SDI	—	Silt density index
SE	—	Standardized effects
SGS	—	Steam generation system
SS	—	Sum of squares
TDS	—	Total dissolved solids
VIF	—	Variance inflation factor
WTP	—	Water treatment plant
X	—	Dimensionless coded factors of parameters
X_1	—	pH
X_2	—	Antiscalant concentration
X_3	—	Flow rate
X_4	—	Redox potential
Y	—	Response
Y_1	—	Conductivity rejection rate
Y_2	—	Calcium rejection rate
Y_3	—	Magnesium rejection rate
Y_4	—	Transmembrane pressure

References

[1] Y. Hamed, R. Hadji, B. Redhaounia, K. Zighmi, F. Bâali, A. El Gayar, Climate impact on surface and groundwater in North Africa: a global synthesis of findings and recommendations, Euro-Mediterr. J. Environ. Integr., 3 (2018) 1–15.

[2] N. El Assaoui, A. Sadok, I. Merimi, Impacts of climate change on Moroccan's groundwater resources: state of art and development prospects, Mater. Today:. Proc., 45 (2021) 7690–7696.

[3] F. Zaviska, L. Zou, Using modelling approach to validate a bench scale forward osmosis pre-treatment process for desalination, Desalination, 350 (2014) 1–13.

[4] N.X. Tsiourtis, Desalination and the environment, Desalination, 141 (2001) 223–236.

[5] Q. Zhao, D.L. Zhao, T.S. Chung, Thin-film nanocomposite membranes incorporated with defective ZIF-8 nanoparticles for brackish water and seawater desalination, J. Membr. Sci., 625 (2021) 119158, doi: 10.1016/j.memsci.2021.119158.

[6] L.F. Greenlee, D.F. Lawler, B.D. Freeman, B. Marrot, P. Moulin, Reverse osmosis desalination: water sources, technology, and today's challenges, Water Res., 43 (2009) 2317–2348.

[7] J. Kucera, Reverse Osmosis: Industrial Processes and Applications, 2nd ed., Scrivener Publishing, Salem, Massachusetts, 2015.

[8] N. El Qacimi, N. El Baraka, N. Saffaj, R. Mamouni, A. Laknifli, S. Alami Younssi, A. Faouzi, H. Zidouh, Preparation and characterization of flat membrane support based on Sahara Moroccan clay: application to the filtration of textile effluents, Desal. Water Treat., 143 (2019) 111–117.

[9] Y.-N. Wang, R. Wang, Chapter 1 – Reverse Osmosis Membrane Separation Technology, A. Fauzi Ismail, M.A. Rahman, M.H. Dzarfan Othman, T. Matsuura, Eds., Membrane Separation Principles and Applications. From Material Selection to Mechanisms and Industrial Uses, Handbooks in Separation Science, Elsevier, Amsterdam, Netherlands, 2019, pp. 1–45.

[10] S. Jiang, Y. Li, B.P. Ladewig, A review of reverse osmosis membrane fouling and control strategies, Sci. Total Environ., 595 (2017) 567–583.

[11] M. Ansari, M.A. Al-Obaidi, Z. Hadadian, M. Moradi, A. Haghighi, I.M. Mujtaba, Performance evaluation of a brackish water reverse osmosis pilot-plant desalination process under different operating conditions: experimental study, Cleaner Eng. Technol., 4 (2021) 100134, doi: 10.1016/j.clet.2021.100134.

[12] DOW, Water & Process Solutions, FILMTEC™ Reverse Osmosis Membranes: Technical Manual, Midland MI, USA, 2013.

[13] J. Ferry, B. Widyolar, L. Jiang, R. Winston, Solar thermal wastewater evaporation for brine management and low pressure steam using the XCPC, Appl. Energy. 265 (2020) 114746, doi: 10.1016/j.apenergy.2020.114746.

[14] Z. Jokadar, C. Ponte, Ouarzazate Solar Power Complex, Phase 1 Morocco Specific Environmental and Social Impact Assessment, Vol. 1, ACWA Power, Ouarzazate, Morocco, 2013.

[15] M.S. Ben Fares, S. Abderafi, Water consumption analysis of Moroccan concentrating solar power station, Sol. Energy, 172 (2018) 146–151.

[16] A. Azouzoute, M. El Ydrissi, Z. Elmaazouzi, M. Benhaddou, M. Salihi, C. Hajjaj, M. Garoum, Thermal production and heat cost analysis of the potential of solar concentrators for industrial process applications: a case study in six sites in Morocco, Sci. African, 12 (2021) 765, doi: 10.1016/j.sciaf.2021.e00765.

[17] Y.L. He, K. Wang, Y. Qiu, B.C. Du, Q. Liang, S. Du, Review of the solar flux distribution in concentrated solar power: non-uniform features, challenges, and solutions, Appl. Therm. Eng., 149 (2019) 448–474.

[18] N.A. Moharram, S. Bayoumi, A.A. Hanafy, W.M. El-Maghlany, Hybrid desalination and power generation plant utilizing multi-stage flash and reverse osmosis driven by parabolic trough collectors, Case Stud. Therm. Eng., 23 (2021) 100807, doi: 10.1016/j.csite.2020.100807.

[19] A. Wang, J. Liu, S. Zhang, M. Liu, J. Yan, Steam generation system operation optimization in parabolic trough concentrating solar power plants under cloudy conditions,

Appl. Energy, 265 (2020) 114790, doi: 10.1016/j.apenergy.2020.114790.

[20] J.J.C.S. Santos, J.C.E. Palacio, A.M.M. Reyes, M. Carvalho, A.J.R. Freire, M.A. Barone, Concentrating Solar Power, in: Adv. Renew. Energies Power Technol., Elsevier, Amsterdam, Netherlands, 2018, pp. 373–402.

[21] O. Ogunmodimu, E.C. Okoroigwe, Concentrating solar power technologies for solar thermal grid electricity in Nigeria: a review, Renewable Sustainable Energy Rev., 90 (2018) 104–119.

[22] M. Alguacil, C. Prieto, A. Rodriguez, J. Lohr, Direct steam generation in parabolic trough collectors, Energy Procedia, 49 (2013) 21–29.

[23] N. Voutchkov, Chapter 6 – Conditioning of Saline Water, N. Voutchkov, Ed., Pretreatment for Reverse Osmosis Desalination, Elsevier, Amsterdam, Netherlands, 2017, pp. 113–135.

[24] J. Kavitha, M. Rajalakshmi, A.R. Phani, M. Padaki, Pretreatment processes for seawater reverse osmosis desalination systems—a review, J. Water Process Eng., 32 (2019) 100926, doi: 10.1016/j.jwpe.2019.100926.

[25] M. Badruzzaman, N. Voutchkov, L. Weinrich, J.G. Jacangelo, Selection of pretreatment technologies for seawater reverse osmosis plants: a review, Desalination, 449 (2019) 78–91.

[26] C. Otero, A. Urbina, E.P. Rivero, F.A. Rodríguez, Desalination of brackish water by electrodeionization: Experimental study and mathematical modeling, Desalination, 504 (2021) 114803, doi: 10.1016/j.desal.2020.114803.

[27] S.L.C. Ferreira, Experimental Design, in: International Encyclopedia of Human Geography, 3rd ed., Elsevier, 2018, pp. 672–675.

[28] Q.H. Le, P.J.T. Verheijen, M.C.M. van Loosdrecht, E.I.P. Volcke, Experimental design for evaluating WWTP data by linear mass balances, Water Res., 142 (2018) 415–425.

[29] M. Chérif, I. Mkacher, L. Dammak, A. Ben Salah, K. Walha, V. Nikonenko, S. Korchane, D. Grande, Fractional factorial design of water desalination by neutralization dialysis process: concentration, flow rate, and volume effects, Desal. Water Treat., 57 (2016) 14403–14413.

[30] S.M. Riley, D.C. Ahoor, K. Oetjen, T.Y. Cath, Closed circuit desalination of O&G produced water: an evaluation of NF/RO performance and integrity, Desalination, 442 (2018) 51–61.

[31] K.D. Demadis, S.D. Katarachia, Metal-phosphonate chemistry: synthesis, crystal structure of calcium-amino-TRIS-(methylene phosphonate) and inhibition of $CaCO_3$ crystal growth, Phosphorus, Sulfur Silicon Relat. Elem., 179 (2004) 627–648.

[32] M. Di Martino, S. Avraamidou, J. Cook, E.N. Pistikopoulos, An optimization framework for the design of reverse osmosis desalination plants under food-energy-water nexus considerations, Desalination, 503 (2021) 114937, doi: 10.1016/j.desal.2021.114937.